REDUCING CHANNEL FLOW ENERGY LOSSES USING DEFLECTORS

Sanjin FUĆAK, Zoran ČARIJA, Zoran MRŠA

Tehnički fakultet, Vukovarska 58, Tel: +385(0)51 651554
sanjinf@riteh.hr, zcarija@riteh.hr, mrsa@riteh.hr

Abstract: This paper gives an overview of the optimization process for deflector shape design. The task was to lower the water level in the S-shaped outflow channel of HPP Vinodol by steadying the flow and reducing energy losses. Parameterized designs of ten deflectors were optimized using a genetic algorithm that evaluated each setup by running a 2D fluid flow simulation. After analyzing total pressure losses in channel segments, optimal designs were chosen according to total pressure loss and flow uniformity throughout the channel. The resulting best case design set showed a 37% reduction in energy losses over the worst-case representation of the actual channel. This provides a solid basis for further simulations using a 3D fluid flow numerical model of the channel. The 3D simulation based on the best 2D case design set showed a significant decrease in spillage through the channel ceiling into the above engineering room.

1 INTRODUCTION

The HPP Vinodol houses six Pelton turbines with a combined water flow originally set at 17.4 [m3/s] which was increased to 18.7 [m3/s] with the new runners. The uniquely S-shaped drainage channel that collects the water from the turbines was designed for a much lower throughput and has a suboptimal shape that causes turbulences in water flow and raises the water level above the ceiling [1].

The rising water level under the turbines, caused by flow losses within the channel, is controlled by pumping air into the turbine housing. When the plant operates with maximal power output, the water enters the engine room through its drainage ducts which become channel ceiling water vents. The newer turbine runners raised the water flow so that the drainage capabilities of the channel were found inadequate and a solution was sought in order to reduce the water level.

2 COMPUTATIONAL MODEL

2.1 Geometrical S-channel model and mesh

The channel was modeled according to available original designs. Corrections were introduced after a visit to the S-channel in which photographs and measurements of characteristic points were taken. The resulting 3D model was imported into the mesher as a geometrical base for the creation of the computational grid in 3D and 2D fluid flow simulations which were performed in Fluent 6.2.16. Design restrictions prohibited altering the walls in the existing channel geometry due to their armature and the impact on structural integrity of the engineering room above, so the changes have to be added onto the walls. Additional improvements of the model were introduced after a second visit and used for the 3D fluid flow simulation.

The mesh used in the 2D model was an unstructured grid of triangle elements, the initial 3D model used the unstructured tetrahedral mesh and later 3D models used a hybrid mesher of structured hexahedral and unstructured tetrahedral sections.

2.2 Deflector parameterization and simulation setup

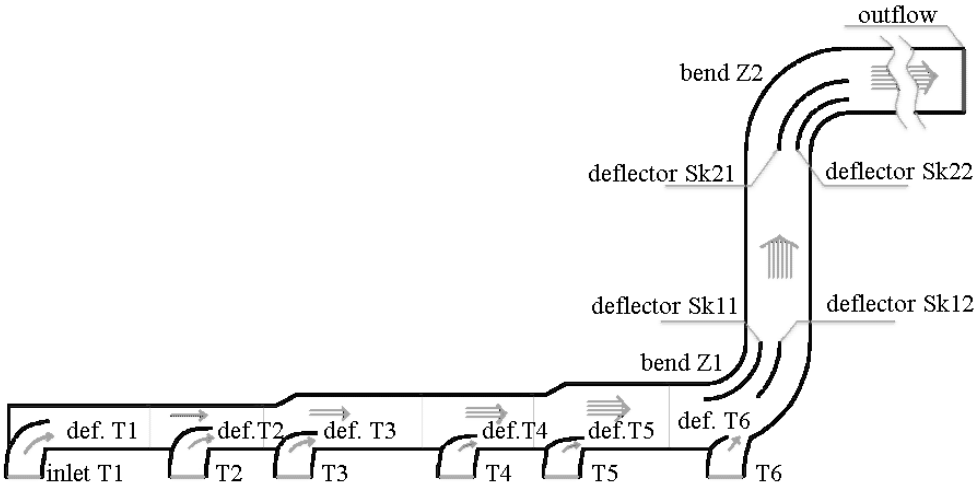

Figure1: Designations of computational channel model elements including deflectors

The first 3D fluid flow simulation of the actual channel was used to highlight the problem zones through examined streamlines and particle tracks. A 2D intersection in the model Z-plane was chosen as the optimization domain, level with the middle of the trapezoidal T1 through T6 velocity inlets at a height of 1.7 m inside the channel. The small cooling water inflow upstream from inlet T1 was walled-off and the domain outflow was set 12m after the Z2 bend. The simplification of the 3D domain to a 2D section allowed an efficient comparison of a greater number of deflector setups leaving only the comparatively good ones as candidates for later time-consuming 3D simulations.

Taking into account the results obtained in the study [2], the Sk11 through Sk22 deflectors were initially positioned according to elbow deflector guidelines set in [3].

The first design of the *T1* through *T6* deflectors was set to follow the streamlines and smoothed contours of the channel widening from 2m to 2.5m at the *T3* inlet and 2.5m to 3m at the *T5* inlet. The widening occurs rather steeply in the actual channel.

A 2D unstructured mesh was used with wall element sizes set to 10 mm and maximum element size set to 140 mm with a 60% growth bias towards wall element size. The k-ε turbulent viscosity model was selected for Fluent simulations [4] and the residual convergence criterion was fixed at 10E-4. Adaptions were not used as they crashed the scripted simulations of various setups unpredictably.

Individual optimization of sections around each T-deflector had shown that the variations in general shape had a lesser impact on energy losses than the aperture of the deflector measured from the right-hand channel wall. The design parameters for deflectors *T1* through *T5* were therefore the distance of the deflector tip from the right-hand wall Δ(x) and Δ(y) from the origin for *T6*. The circular arc *Sk11* and *Sk12* deflectors were defined by their distance from the convex left-hand side of the Z1 bend Δ(R). The actual contours of the T-deflectors were left for a 3D optimization and were set along the actual-state streamlines for the pre-generated case mesh. The deflectors *Sk22* and *Sk23* remained in their original positions

2.3 Genetic algorithm (GA) and optimization automation

The genetic algorithm (GA) for an external fitness function with variables for each deflector parameter was compiled from the GALOPPS GA libraries using roulette wheel selection, crossover and mutation [5], [6]. The GA encoded each parameter as a binary gene forming chromosomes that represented each deflector setup. Their fitness function variable was set as the difference of total pressure in the whole channel (between all model inlets and the outlet) and was calculated in a custom application written in C++, outlined in Fig. 2. This application initialized and monitored the meshing, CFD simulation and gathered statistics before returning the fitness value to the GA executable.

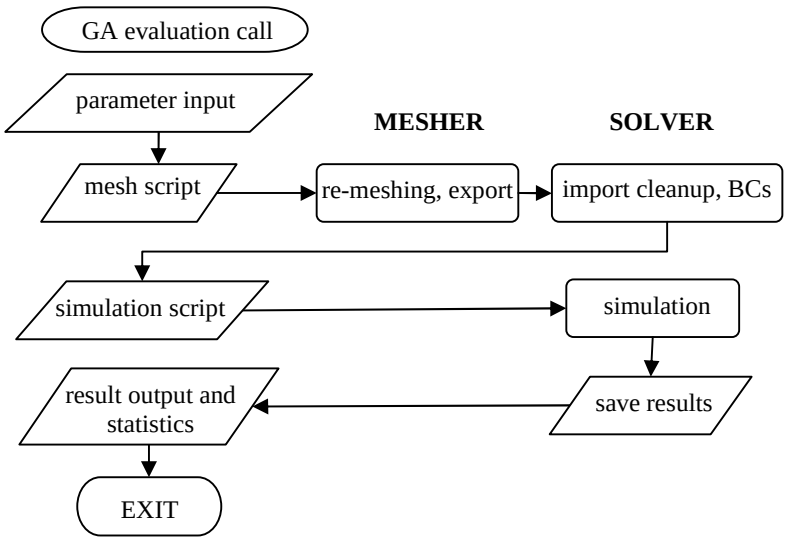

Figure2: Block diagram for for a single evaluation with the fitness function application showing external calls to the mesher and solver

The use of a pre-generated case mesh considerably sped up the meshing part of each evaluation. The meshing script recalculated the deflector shape from coordinates selected by the GA and altered the case mesh accordingly before exporting it for Fluent. The application then generated the script to run the Fluent simulation and extract data from result transcripts or output graphical representations for post processing.

A file with all the models, parameters and results was maintained in the local run directory so the GA fitness evaluation calls were checked versus existing previously evaluated parameter set results to prevent duplicate simulations. This also enabled GA runs to continue after computer crashes or the manual aggregation of results from GA runs on several different machines.

As the total pressure loss sometimes differed little with varying deflector positions, the uniformity of velocity magnitude throughout the channel was taken into account as an additional control value. This was expressed through the area surface with velocities greater than 4.5 [ms^{-1}] as mass flow remained constant in all case variations.

3 DESIGN OPTIMIZATION THROUGH 2D SIMULATIONS

3.1 3.1 Simulation of the actual state

The inlet velocity boundary conditions were set at the same value of 1.41 [ms^{-1}] taken from a uniform flow field in the trapezoidal inlet cross section of the 3D channel model with the maximum inflow of 3.12 [m^3/s] from each turbine. With the unit control volume height used in Fluent this gives the total volume flow through the 2D section as 11.45 [m^3/s] as opposed to the 18.7 [m^3/s] in the actual 3D case of the whole channel.

3.2 Optimization phases

The optimization was performed in several phases changing the focus of attention in order to determine the most influential parameters, i.e. deflectors, in the simulation.

In the first phase, zero-thickness deflectors were optimized individually for each T-segment, always taking the upstream portion of the channel into account. Due to the upstream influence of each deflector, the local simulation results for deflectors differed from results obtained after attaching downstream channel segments.

The second phase consisted of optimizing the part of the channel upstream from the bend *Z1*, including segments *T1* through *T5*.

The whole channel was modeled in the third phase using best-case positions from the previous phase and varying the positions of *T6*, *Sk11* and *Sk12* in the Z1 bend.

The fourth phase optimized the whole channel again, but varied all the parameters within smaller value ranges as the beneficial ranges were obtained from the second and third phase.

3.3 Final 2D optimization results

The final phase of 2D simulations at the channel mid-height used a changed deflector design. The previous instances used simplified zero-thickness T-junction deflectors, and here they were given width with an outer edge that sweeps seamlessly into the channel

wall upstream of the T-junction and is elongated over the downstream edge of the T-junction. The outer edge was needed to smooth the fluid flow and avoid swirl zones where deflectors decrease channel width. The scripted deflector tip coordinate adjustment for different setups was adjusted so that the two deflector edges don't overlap despite blade-thin tips. The outer edge was defined by a spline curve through four points and the inner edge through three. Additional curvature constraints were set in the splines in order to preserve the streamline of the deflectors. The mesh was further improved by refining the elements around each tip to improve the representation of the wake and the confluence of inlet streams from *T1* to *T5* into the main channel flow. The tip of the *T6* deflector was inverted and inclined towards the channel because the main flow choked the inflow from turbine *T6*.

The increases in channel width at *T3* and *T5* were smoothed with a splined transition complementary to the deflector outer edge in order to further improve flow stability and reduce losses, resembling their dimensions in the original designs which differ greatly from their actual state. The inner edge of each T-deflector overlapped the lip in the left-hand side of the T-inlet which has a concave sweep and would otherwise slow the stream creating slowdown and an uneven inflow.

Due to these significant design changes, a number of simulations were run with larger steps in deflector parameters in order to again determine the most influential ones and their beneficial ranges. T4 through T6, as well as Sk11 and Sk12 have shown to be the dominant parameters, so positions T1 through T3 were fixed according to best results and the dominant parameters were varied in simulations on a multiprocessor system within smaller ranges and a finer step:

The simulation results for the best case showing the smallest pressure loss and the smallest area of velocities less than 4.5 [m/s] were obtained for the following parameters:

Table 1: Design parameters for the final 2D optimization best case

	Δx					**Δy**	**ΔR**	
Deflector	**T1**	**T2**	**T3**	**T4**	**T5**	**T6**	**Sk11**	**Sk12**
[mm]	1800	1000	830	630	590	1250	700	1380

Table 2: Specific total energy losses in S-channel segments for the 2D simulations of the original actual channel state and the 2D optimization best case models computed from surface integrals of mass averaged values

Segment	**T1 .. T2**	**T2 .. T3**	**T3 .. T4**	**T4 .. T5**	**T5 .. Z1**	**Z1+T6**	**Z1 .. Z2**	**Z2**	**Z2 .. out**	**TOTAL**
ORIGINAL Loss [W]	812	1326	1867	2796	3630	19082	709	8859	478	39557
OPTIMIZED Loss [W]	385	1239	1612	2726	3728	6533	2280	3740	2704	24947

The comparison of results in Table 2 shows a significant reduction in losses of 37% when using deflectors. The losses in the *Z1* bend (including the *T6* inlet) are reduced by 65%, and in the *Z2* bend by 57%. The increased losses in the section between the *Z1* and

Z2 bends (influenced by the wake from *Sk11* and *Sk12* deflectors), as well as local total pressure increases at velocity inlets, are less significant than the overall loss reduction.

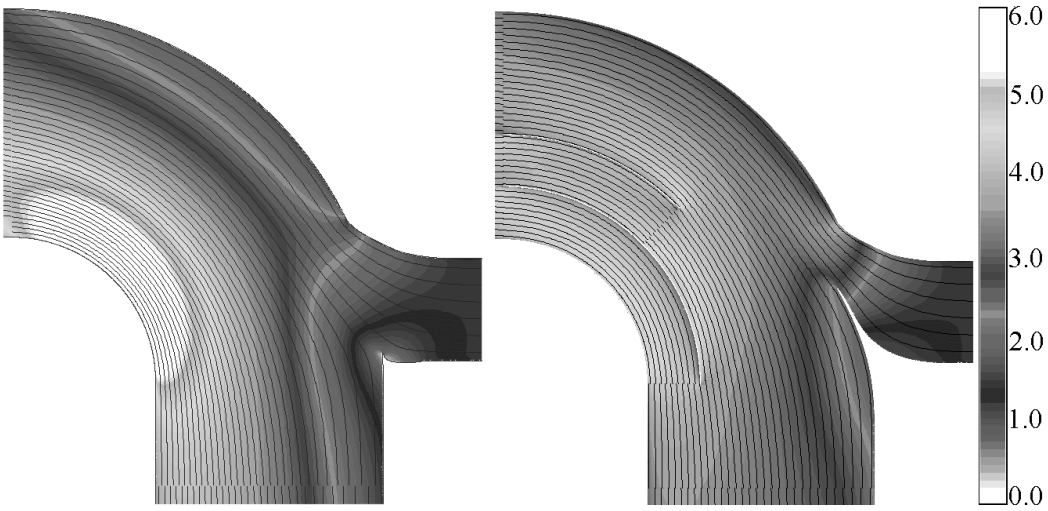

Figure3: Velocity magnitudes in the Z1 bend (shaded areas, legend in [ms^{-1}]) with superimposed streamlines (black curves); showing the original channel state (left) and optimization best case deflectors (right)

4 VOF 3D MODEL

A 3D [4, 7] model using the best case deflector design, extruded vertically from bottom to ceiling, was used to analyze the spillage in the engineering room. The three vents in the channel ceiling were connected to a simplified representation of the room above in order to compute the water level in the steady-state solution. The vents are positioned aligned with the generators, halfway between turbine outflow segment pairs T1 and T2, T3 and T4, T4 and T5.

The predominantly hexahedral 3D mesh was generated with a thin shell hexahedral layer on all solid surfaces in order to improve boundary layer computations. The final mesh had about 1.5 million cells.

The Volume of Fluid (VoF) model with water liquid and air phases was used to obtain the free surface. The realizable k-ε viscous model was selected for its robustness and speed of execution.

The simulation showed a significant decrease in the engineering room water level from 120-170 [mm] in the original state to under 30 [mm] in the channel with deflectors. Fig. 4 and 5 show the water height profiles at three characteristic cross sections of the engineering room positioned through the middle of turbine outflow segments T2, T4 and T6. The visual difference in those water levels is shown in Fig. 6.

The free surface in the channel flow did not form until the Z2 bend (Fig. 7). The ceiling height there sharply arches above 2.6 [m], right after the service entrance opening in Z2.

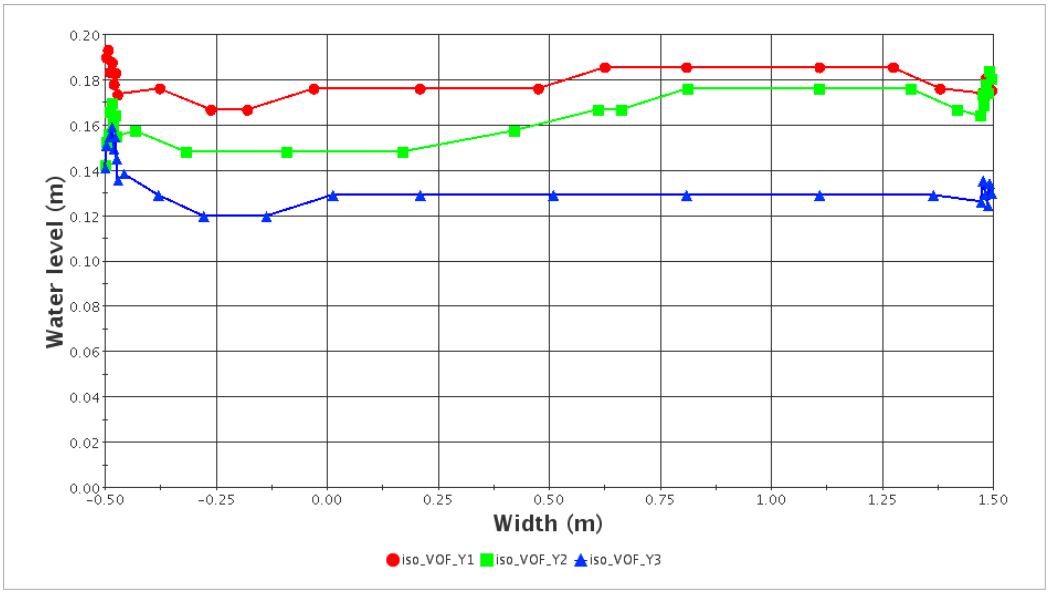

Figure4: Water level height in the engineering room of the original channel state, measured at characteristic cross sections

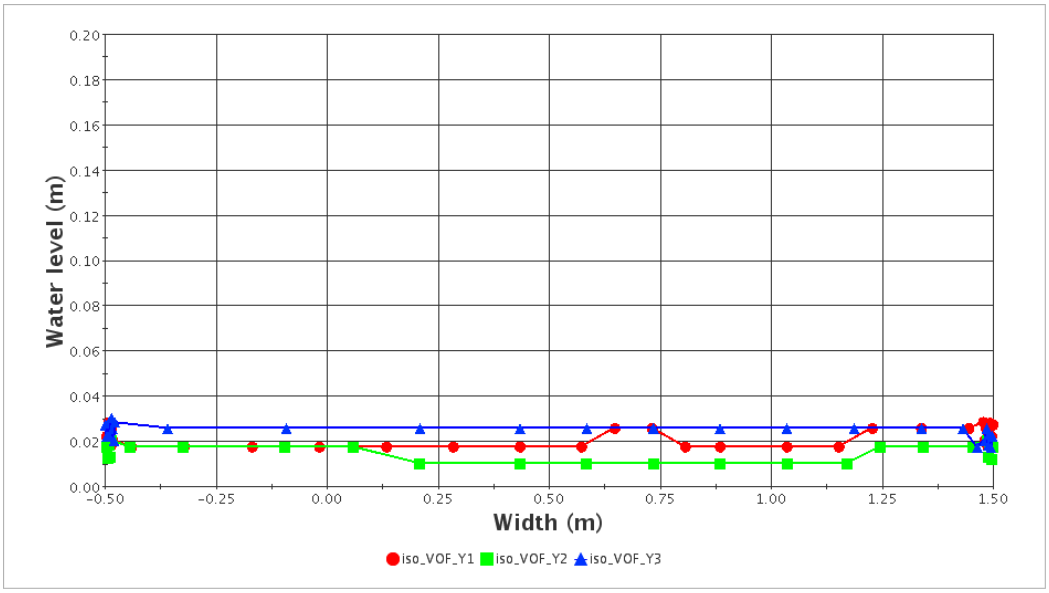

Figure5: Water level height in the engineering room in the channel model with deflectors, measured at characteristic cross sections

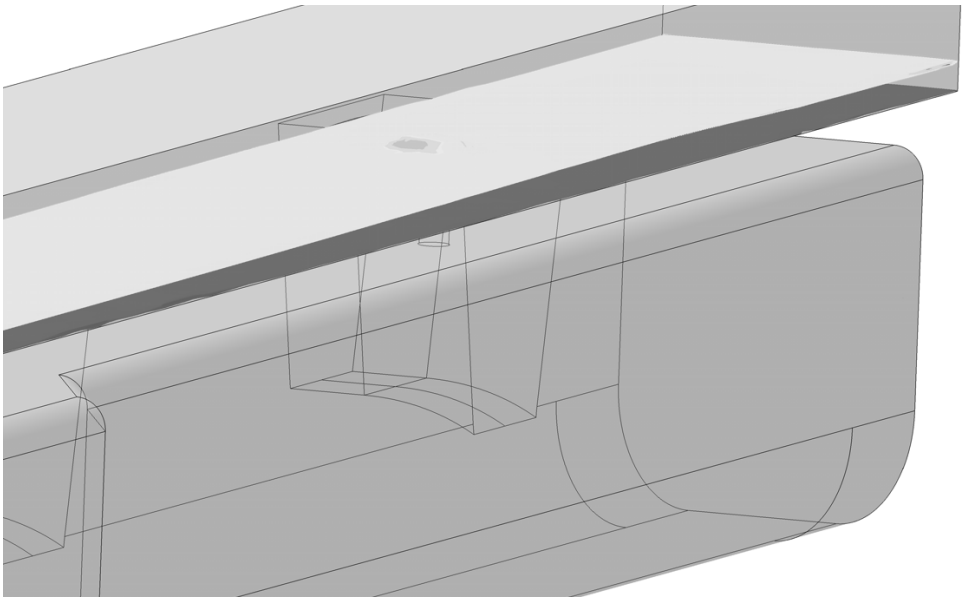

Figure6: Water level in the engineering room with deflectors (dark surface) and without them (light surface above) shown on a simplified 3D model of the original channel

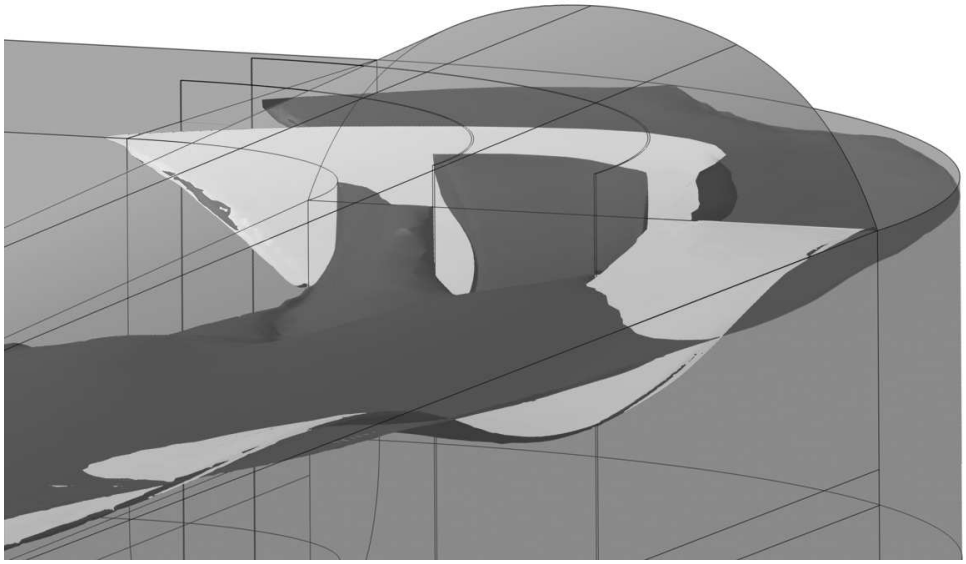

Figure7: Free surface in the Z2 bend with deflectors (dark surface) and without them (light surface intersecting) shown on a simplified 3D model of the original channel with *Sk21* and *Sk22* deflector outlines

5 CONCLUSION

The 2D optimization results show more uniformity in the velocity field, eliminating the high-velocity zone in the Z1 bend of the original state, as shown in Figure 4. The resulting reduction in total pressure loss and related energy losses of 37% is considerable.

The 3D simulation has shown a significant reduction of the water level in the engineering room showing the usefulness of deflectors even in their basic form.

Future research should use the 3D fluid flow model for optimization in order to capture the swirl and gravitational influences in the flow more accurately and optimize the shape of the deflectors along the Z-axis. A structural analysis of forces and strains in the material of the deflectors under maximum turbine output would be needed as well as the analysis of dynamic stresses during load cycling. Verification of 3D CFD results using a scale model of the channel would be important before making deflector prototypes for installation in the actual channel.

REFERENCES

[1] R. Belobrajić, D. Marjan, H. Zibar, *Analiza rezultata mjerenja hidrauličkih gubitaka odvodnih organa HE "Vinodol"*. HE Vinodol, Tribalj, 1992.

[2] Z. Mrša, Z. Čarija. *Analiza mogućnosti smanjenja hidrauličkih gubitaka odvodnog kanala HE "Vinodol"*. Tehnički fakultet u Rijeci, Rijeka, 2005.

[3] I. E. Idel'cik. *Handbook of Hydraulic Resistance*. Israel Program for Scientific Translation, Jerusalem, 1966.

[4] F. H. Ferziger, M. Perić. *Computational Methods for Fluid Dynamics*. Springer Verlag, Berlin, 2002.

[5] D. E. Goldberg. *Genetic Algorithms in Search, Optimization and Machine Learning*. Addison-Wesley Publishing Company Inc, Boston, 1989.

[6] E. D. Goodman. *An Introduction to GALOPPS The "Genetic ALgorithm Optimized for Portability and Paralellism" System*. Michigan State University, East Lansing, 1996.

[7] H.K. Versteeg, W. Malalasekera, *An Introduction To CFD The Finite Volume Method*, ISBN 0-582-21884-5, Longman Gr., 1995.